# The Basal Keratin Network of Stratified Squamous Epithelia: Defining K15 Function in the Absence of K14

**Catriona Lloyd, Qian-Chun Yu, Jian Cheng, Kursad Turksen, Linda Degenstein, Elizabeth Hutton, and Elaine Fuchs**

Howard Hughes Medical Institute, Department of Molecular Genetics and Cell Biology, The University of Chicago, Chicago, Illinois 60637

***Abstract.*** Keratin 5 and keratin 14 have been touted as the hallmarks of the basal keratin networks of all stratified squamous epithelia. Absence of K14 gives rise to epidermolysis bullosa simplex, a human blistering skin disorder involving cytolysis in the basal layer of epidermis. To address the puzzling question of why this disease is primarily manifested in skin rather than other stratified squamous epithelia, we ablated the K14 gene in mice and examined various tissues expressing this gene. We show that a key factor is the presence of another keratin, K15, which was hitherto unappreciated as a basal cell component. We show that the levels of K15 relative to K14 vary dramatically among stratified squamous epithelial tissues, and with neonatal development. In the absence of K14, K15 makes a bona fide, but ultrastructurally distinct, keratin filament network with K5. In the epidermis of neonatal mutant mice, K15 levels are low and do not compensate for the loss of K14. In contrast, the esophagus is unaffected in the neonatal mutant mice, but does appear to be fragile in the adult. Parallel to this phenomenon is that esophageal K14 is expressed at extremely low levels in the neonate, but rises in postnatal development. Finally, despite previous conclusions that the formation of suprabasal keratin filaments might depend upon K5/K14, we find that a wide variety of suprabasal networks composed of different keratins can form in the absence of K14 in the basal layer.

KERATINS belong to the superfamily of intermediate filament (IF)[1] proteins, which have the remarkable capacity to assemble into 10-nm filaments in vitro, in the absence of any auxiliary proteins or factors (for review, see Fuchs and Weber, 1994). Keratins are divided into two sequence types, both of which share a common, largely α-helical secondary structure, capable of forming coiled coil heterodimers, which then further assemble to form obligatory heteropolymers. Type I keratins include K9-K20 (63–40 kD), and type II keratins encompass K1–K8 (67–53 kD) (Moll et al., 1982*a*). While most combinations of type I and type II keratins can copolymerize in vitro (Franke et al., 1983), keratins are often coexpressed as specific pairs in vivo (Sun et al., 1984).

Mitotically active keratinocytes of all stratified squamous epithelia express K5 and K14 (Nelson and Sun, 1983; Byrne et al., 1994). As cells differentiate, they often downregulate transcription of K5/K14 and induce new sets of differentiation-specific keratins which vary among stratified tissues (Fuchs and Green, 1980; Moll et al., 1982*a*; Stellmach et al., 1991). In epidermis and forestomach (mouse), differentiating cells express K1 and K10 (Fuchs and Green, 1980; Roop et al., 1987; Schweizer et al., 1988). K6 and K16 are expressed in a variety of differentiating cells, including the outer root sheath (ORS) of hair follicle and the dorsal spikes of tongue (Moll et al., 1982*a*; Rentrop et al., 1986). K6 and K16 are also unusual in that they are induced suprabasally under certain conditions that include epidermal hyperproliferation (Sun et al., 1984; Mansbridge and Knapp, 1987). In differentiating cells of esophagus, K4 and K13 are induced (Fuchs and Green, 1980; Moll et al., 1982*a*; van Muijen et al., 1986), and in cornea, K3 and K12 are expressed (Moll et al., 1982*a*; Wu et al., 1994).

It has been suggested that the overall function of epidermal keratin filaments is to impart mechanical integrity to the cells, without which, the cells become fragile and prone to rupturing. This notion was initially proposed on the basis of transgenic mice expressing a truncated K14 gene which produced the pathological features of epidermolysis bullosa simplex (EBS), in which basal epidermal cells show keratin IF aggregations and lyse upon mechani-

Jian Cheng and Kursad Turksen contributed equally to this work.

Address all correspondence to Dr. Elaine Fuchs, Dept. of Molecular Genetics and Cell Biology, Howard Hughes Medical Institute, The University of Chicago, Chicago, IL 60637. Fax: (312)702-0141.

1. *Abbreviations used in this paper*: EBS, epidermolysis bullosa simplex; EH, epidermolytic hyperkeratosis; EPPK, epidermolytic palmoplantar keratoderma; ES, embryonic stem; IF, intermediate filament; NGS, normal goat serum; ORS, outer root sheath; rt, room temperature.

cal trauma (Vassar et al., 1991; Coulombe et al., 1991*b*). Subsequently, mice expressing a truncated K10 gene were also generated and shown to exhibit features of epidermolytic hyperkeratosis (EH), which is similar to EBS, but a disorder of suprabasal rather than basal cells (Fuchs et al., 1992). In humans, EBS and EH are generally autosomal dominant disorders, and keratin gene mutations have been detected in DNAs from patients with EBS (K5 and K14 mutations), EH (K1 and K10 mutations) and epidermolytic palmoplantar keratoderma (EPPK; K1 and K9 mutations) (Bonifas et al., 1991; Coulombe et al., 1991*a*; Cheng et al., 1992; Chipev et al., 1992; Lane et al., 1992; Rothnagel et al., 1992; Reis et al., 1994; Torchard et al., 1994; for review see Fuchs, 1994). The severity of the disease correlates with the degree to which these mutants perturb IF assembly in vitro (Coulombe et al., 1991*b*; Cheng et al., 1992; Chipev et al., 1992; Letai et al., 1993).

Although autosomal dominant, i.e., dominant negative, mutations do not allow unequivocal assignment of function, it was recently shown that patients homozygous for a premature termination codon in their K14 gene do not have detectable K14-K5 keratin networks and yet have severe EBS (Chan et al., 1994; Rugg et al., 1994). While demonstration of function still awaits the creation of true K14 null mutations, these data provide further support for the notion that cell fragility is a consequence of the absence of a major keratin filament network, rather than the presence of insoluble aggregates of improperly polymerized keratin. Given the presumed general importance of the K14-K5 network among stratified squamous epithelial tissues, it is odd that ablation or mutation of K14 produces a disease that is largely manifested in the skin. Although not formally tested, the prevailing notion is that internal stratified squamous epithelial tissues are more protected from mechanical stress than epidermis (Fuchs, 1994; Anton-Lamprecht, 1994). This issue rests at the crux of the functional significance of keratin filaments.

A clue that there might be additional explanations underlying the relatively mild effects of K14 mutations and/or ablation on other stratified squamous epithelia came from biochemical and electron microscopy studies on the two recessive EBS patients that seemingly lacked K14 (Rugg et al., 1994; Chan et al., 1994). These patients still had appreciable levels of K5, which was surprising, since studies in fibroblasts had shown that in the absence of its partner, a keratin is unstable and rapidly turns over (Kulesh and Oshima, 1988; Lersch et al., 1989). Rugg et al. (1994) proposed that the K5 protein might be stabilized by association with the plasma membrane. Chan et al. (1994) suggested that K5 might be stabilized by a second, as yet unidentified type I keratin which then forms a lesser, but bona fide, keratin filament network in basal cells. One contender for K5 stabilization is K15, known to exist in minor amounts in the adult epidermis (Moll et al., 1982*b*) and in some other stratified epithelia (Moll et al., 1982*a*). While little is known about the location of this keratin in these tissues, and while monospecific antibodies are not yet available, a K15 cRNA probe has been shown to hybridize to all layers of esophagus (Leube et al., 1988).

If there are two potential partners for K5, then this would add a new complexity to our understanding of the consequences of K14 mutation and/or ablation in mice and in humans. Moreover, it would raise new questions about the functional significance of the multiplicity of keratins and about the effects of changing the ratio of the two type I keratins among various epithelial tissues. Finally, in vitro studies have provided some evidence to suggest that the basal keratin pair, K5 and K14, serves as an essential foundation for building K1 and K10 filaments (Kartasova et al., 1993). Is it true that in vivo, the formation of different suprabasal keratin networks of stratified tissues is dependent upon the preexisting keratin filament network of basal cells? If so, what is the relative importance of a K5-K15 network versus a K5-K14 network in the basal layer?

To begin to explore these issues of keratin function and the significance of the complex expression patterns of keratins in stratified epithelia, we have used embryonic stem cell technology to engineer mice ablated for the K14 gene. We show that the levels of residual keratin filaments within the basal cells of different stratified tissues from these mice vary dramatically. To analyze these residual keratin networks, we made a monospecific antiserum against K15. We show that K15 is indeed a third, and sometimes major, component of the basal keratin network of stratified epithelia, and that the ratio of K14/K15 can change dramatically during postnatal development. Moreover, K15 is able to assemble into keratin filament networks with K5 in the absence of K14. Finally, these animals have enabled us to evaluate the relative importance of a preexisting basal keratin network on the formation of suprabasal keratin networks. Our findings provide interesting new insights into keratin networks and their functions.

## Materials and Methods

### Screening a 129/sv Genomic Library

A radiolabeled 683-bp fragment encompassing the 5′ end of the human K14 coding sequence (Hanukoglu and Fuchs, 1982) was used to screen an 129/sv mouse genomic library (Stratagene Inc., Palo Alto, CA). Processed filters were prehybridized at 42°C in a solution containing 50% deionized formamide, 0.02 M Hepes, 5× SSC, 1× Denhardt's mixture, 0.1 mg/ml tRNA, and 0.1 mg/ml denatured salmon sperm DNA. A [$P^{32}$]dCTP radiolabeled probe was made using Stratagene PrimeItII kit, and $2 \times 10^6$ cpm/ml were added to fresh hybridization solution. After 12 h, hybridized filters were then washed with 0.1× SSC and 0.1% SDS, and exposed to x-ray film for 16 h. Four hybridizing clones were identified and subsequently purified. One clone, mK14λ-1, was chosen for further study on the basis of its ability to hybridize with probes corresponding to both the 5′ and the 3′ ends of the K14 human cDNA.

### Southern Blot Analysis of ES Cells and Knockout Mice

A fraction of each surviving colony was incubated for 16 h at 37°C in the presence of TE buffer (1 mM EDTA, 50 mM Tris-HCl, pH 7.5) containing 100 mM NaCl, 1% SDS, and 0.5 mg/ml proteinase K. Proteins were then removed with an equal volume of buffer-equilibrated phenol/chloroform (1:1), followed by precipitation with 200 mM sodium acetate in 95% ethanol. DNAs were resuspended in TE buffer. Mouse tissues were incubated at 65°C for 16 h in the presence of 100 mM Tris-HCl, 1 mM EDTA, 0.5% SDS, and 0.25 mg/ml proteinase K. Potassium acetate was added to 1.25 M before extraction with chloroform. The DNA was then precipitated in 70% ethanol and rinsed in 95% ethanol before resuspension in TE buffer.

### Nucleic Acid Analyses

Genomic DNAs or total mouse skin RNAs (Chomczynski and Sacchi, 1987) were resolved by electrophoresis through agarose or formaldehyde agarose gels, respectively, followed by transfer to Hybond $N^+$ (Amersham

Corp., Arlington Heights, IL) by blotting. The nucleic acids were fixed to the membrane by exposure to UV light using a Stratalinker (Stratagene Inc.). Southern blots were then prehybridized for 1 h at 60°C in a solution of 2× SSC, 1% SDS, 0.5% nonfat milk, 0.75 mg/ml denatured sonicated salmon sperm DNA. Hybridizations were then carried out at 60°C for at least 16 h in a solution of $1 \times 10^6$ cpm/ml radiolabeled probe, 2× SSC, 1% SDS, 0.5% nonfat milk, 0.5 mg/ml denatured sonicated salmon sperm DNA, 10% Dextran Sulfate. Blots were then washed for 30 min each, first with 1× SSC, 0.1% SDS, and then with 0.1× SSC, and 0.1% SDS at 60°C. Northern blots were prehybridized for 30 min in Rapid-hyb buffer (Amersham), and then radiolabeled probe was added and blots were incubated an additional 4 h at 65°C. Blots were then washed for 30 min each, first with 1× SSC, 0.1% SDS, and then twice with 0.5× SSC, 0.1% SDS (except the K5 Northern blot was washed with 0.1× SSC, 0.1% SDS).

### *Ultrastructural Analyses*

Tissues were obtained from the organs of duplicate K14 −/−, +/− and +/+ animals, sacrificed at 2–3 d of age. For conventional transmission electron microscopy, tissues were immediately fixed in 2.5% glutaraldehyde and 4% paraformaldehyde (pH 7.3) solution for 24 h, followed by postfixation with 1% osmium tetroxide for 1 h. After en bloc staining and dehydration with ethanol, the samples were embedded with LX-112 medium (Ladd Research Inc., Burlington, VT). All tissues had been properly oriented to ensure that the entire thickness of epidermis or mucous membrane would be sectioned perpendicular to the normal tissue plane. Semithin sections were stained with toluidine blue. 80-nm ultrathin sections were cut with a diamond knife, mounted on uncoated grids, stained with uranyl acetate and lead citrate, and observed with an electron microscope (JEOL-CXII; JEOL U.S.A. Inc., Peabody, MA) operated at 60 kv.

For immunoelectron microscopy, the methods of Warhol et al. (1985) and Coulombe et al. (1989) were employed with some modifications. The tissues were (*a*) fixed with 2% paraformaldehyde, 0.1% glutaraldehyde in PBS for 6 h, (*b*) dehydrated with ethanol, and embedded with Lowicryl K4M medium (Ladd Research Inc.) at –20°C, and (*c*) polymerized with UV light for 7 d at –20°C. Ultrathin sections were mounted on Formvar/carbon coated nickel grids. All sections were first incubated overnight with polyclonal rabbit antisera monospecific for either keratin 14 (no. 199, 1:200), keratin 5 (1:100), or keratin 15 (1:100), followed by a 45-min incubation with a secondary antibody, 20 nm gold conjugated goat anti–rabbit IgG. All grids were then briefly stained with uranyl acetate and lead citrate, and examined with an electron microscope at 60 kv.

### *Immunoblot Analyses*

Following electrophoretic transfer of SDS-PAGE resolved IF proteins to nitrocellulose, blots were hybridized with primary monospecific anti-keratin antibodies and with either of the following developing methods: horseradish peroxidase-conjugated secondary antibodies followed by chemiluminescence ECL (Amersham) or alkaline phosphatase-conjugated secondary antibodies and color development (Bio Rad Labs., Hercules, CA). In each case the blots were blocked with 5% nonfat milk in phosphate buffered saline (PBS) with 0.5% Tween-20 (Sigma Immunochemicals, St. Louis, MO) for 1 h. The blots were incubated with the primary antibodies for 1 h and then washed 3× for 10 min each in PBS, 0.5% Tween-20. The secondary antibodies were incubated with the blots for 1 h and then washed in PBS, 0.5% Tween-20.

### *K15 Antibody Production*

To generate polyclonal antibodies against K15, a peptide CDGQVVSSH-KREI, corresponding to the carboxy-terminal 12 amino acid residues of human K15 (Leube et al., 1988) was synthesized and coupled through its $NH_2$-terminal cysteine residue to keyhole limpet hemocyanin. For the primary inoculation, 250 mg of the conjugated peptide was emulsified in complete Freund's adjuvant and injected into adult female rabbits, whose sera had been pretested by immunofluorescence analysis to make certain it contained no endogenous keratin antibodies. Antibody production was boosted 3 wk later by injection of 150 mg conjugated peptide emulsified in incomplete Freund's adjuvant. After 10 d, the animals were bled through an ear vein. The antibody titer after the first boost was analyzed on HaCat cells with indirect immunofluorescence. Animals making anti-peptide antibodies were then boosted further with 150 μg of conjugated peptide and serum collected 10–12 d after each boost. The specificity of the antibody was established by immunoblotting.

### *Immunohistochemistry*

Animals were sacrificed, and stratified squamous epithelial tissues were excised and fixed in Bouin's fixation for at least 8 h at room temperature (rt). Tissues were embedded in paraffin and sectioned (5 μm). Sections were either stained with hematoxylin and eosin or subjected to immunohistochemistry using the immunogold enhancement technique (Amersham). After removal of paraffin with organic solvents, sections were rehydrated and incubated with 20% normal goat serum (NGS) in PBS for 1 h at rt. Following this preblocking procedure, sections were then incubated for 1 h with the appropriate dilution of primary antibody in 2% NGS/PBS. Following three 10-min washes in PBS, sections were then treated for 1 h at rt with a 1:40 dilution of colloidal gold-conjugated goat anti–rabbit secondary antibodies in 2% NGS/PBS. Following three 10-min washes in PBS, the antigen-antibody complexes were visualized using the silver enhancement kit (Amersham). Antisera were used at the following dilutions: anti-K14, 1:200; anti-K15, 1:200; anti-K5, 1:200; and anti-K6, 1:400.

## *Results*

### *Isolation of the Mouse K14 Gene*

A clone containing a complete mouse K14 (mK14) gene was isolated from a mouse 129/sv genomic DNA library. To assess whether this clone corresponded to the bona fide mouse K14 gene, and was not a K14 pseudogene (Rosenberg et al., 1988), we engineered an expression vector containing the gene and transiently transfected it into simple epithelial cells. As shown in Fig. 1, the transgene expressed a protein which integrated into the endogenous keratin network, and which was detected by an antiserum monospecific for K14. Thus, the gene encoded a functional K14 protein, and provided strong preliminary evidence that we had isolated the bona fide mouse K14 gene. This was later confirmed.

A restriction map of clone mK14λ-1 is shown in Fig. 2 *a*. The TATA box and ATG start codon were determined by

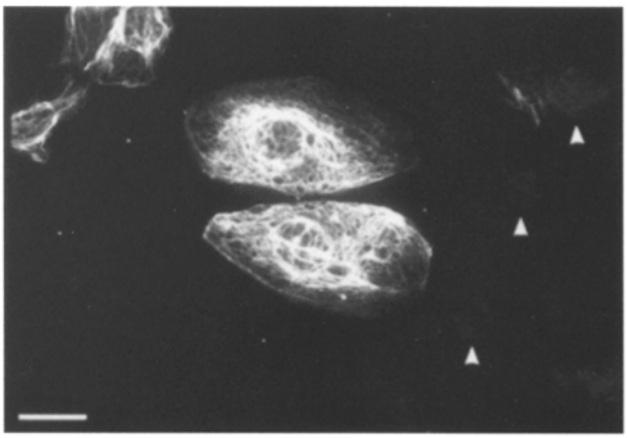

*Figure 1.* Expression of the mouse K14 genomic clone in epithelial cells. The 13-kb SalI fragment containing the mK14 gene was subcloned into the pJay1 vector containing the SV40 promoter and enhancer sequences (Albers and Fuchs, 1987). This vector was introduced into the potoroo kidney epithelial cell line, PtK2, using the calcium phosphate method (Graham and Van der Eb, 1973). 65 h after transfection, the cells were fixed with ice-cold methanol for 10 min. The K14 network was visualized using an anti-K14 peptide antiserum as primary antibody (1:200; Stoler et al., 1988), and an FITC-conjugated secondary antibody. Arrowheads denote cells that were not transfected. Bar, 10 μm.

sequencing (data not shown). Our initial strategy in making a targeting vector was to choose K14 sequences that would allow us to design either a null K14 targeting vector or a replacement vector which could replace the mouse K14 coding sequence with the human vimentin coding sequence. To this end, we chose to target the removal of 1.2 kb of sequence beginning at the ATG codon of the mK14 gene and ending at an EcoRI site within intron I. This strategy gave us the option to insert the full-length human vimentin cDNA at the site of the mK14 translation start codon. At this position, we also inserted a pgk1 promoter-driven neomycin resistance gene for positive selection. Finally, a pgk1-driven Herpes thymidine kinase gene was added at the other end of the targeting vector for negative selection.

The targeting vector DNA was electroporated into embryonic stem (ES) cells derived from the strain 129/Sv, and the transfectants were subjected to positive (G418) and negative (gancyclovir) selection (Hogan et al., 1994). DNAs of surviving colonies were screened for the desired homologous recombinants by Southern blot analysis (Fig. 2 *b*). Of 91 clones analyzed, 17 contained the desired homologous recombination events, and 14 of these were injected into C57BL/6 blastocysts to produce chimeric animals. Three different clones transmitted the mutation through the germline (Fig. 2 *c*), and two lines were bred to homozygosity. In all phases of our study, results were indistinguishable for mice derived from each of the two in-

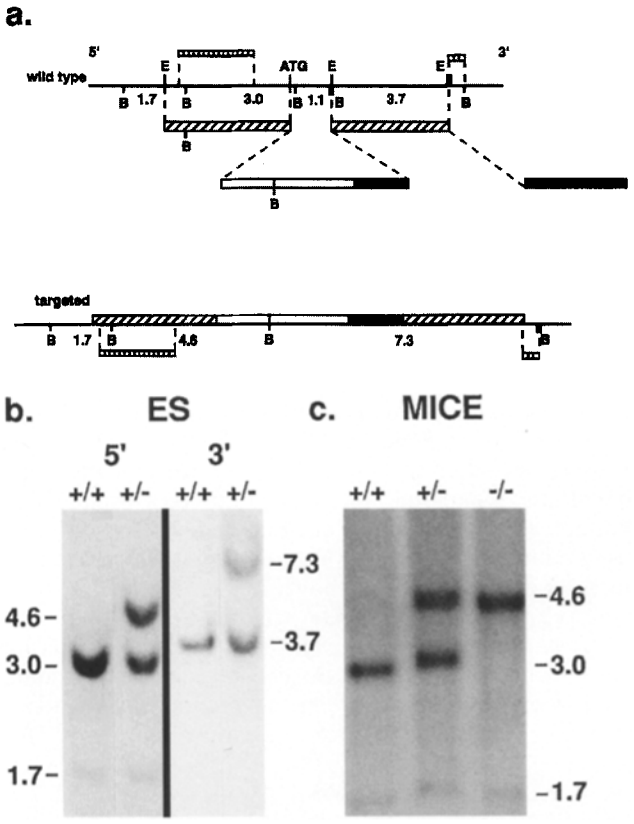


*Figure 2.* Construction of targeting vector and Southern blot analyses to identify homologous recombination events in ES cell lines and ES-derived mice. (*a*) Restriction map of the central region of the mK14λ-1 clone (*top*) and schematic of how the K14 locus should appear when targeted (*bottom*). Cross-hatched boxes, K14 sequences used for targeting vector. The 5′ arm was an EcoR1/Nco1 fragment that began at the ATG translation start codon and extended 3.4-kb 5′ from this point. The 3′ arm was a 3.4-kb EcoR1 fragment which began in intron 1, 1.2-kb 3′ downstream from the ATG start codon of the K14 gene. The white box represents a transgene composed of human vimentin cDNA followed by growth hormone sequences used as a 3′ untranslated segment (see McCormick et al., 1993). This transgene, driven by the endogenous K14 promoter, was never expressed, and hence is irrelevant for the purposes outlined in this paper. Black boxes, pgk1 promoter-driven neomycin resistance gene (5′) and pgk1-driven Herpes thymidine kinase gene (3′). Vertically hatched bars, sequences used as 5′ and 3′ probes for Southern blot analyses. The 5′ probe was a 2-kb HindIII fragment and the 3′ probe was a 0.4-kb EcoR1/BamH1 fragment of the mouse K14 gene. *B*, Bam HI; *E*, Eco RI; *ATG*, K14 translation start codon. Numbers (in kb) represent the distances between Bam HI sites. (*b* and *c*) Representative Southern blot data of Bam HI-digested genomic DNAs isolated from selected ES clones (*b*) or from tail DNAs of mice derived from targeted ES cells (*c*). Examples of the results with 3′ and/or 5′ probes are shown. +/+ denotes two wild-type K14 alleles, +/− denotes one targeted and one wild-type K14 allele, and −/− denotes two targeted alleles. Sizes of hybridizing fragments are indicated in kb. Sizes of all hybridizing fragments were as expected, based on the maps in (*a*).

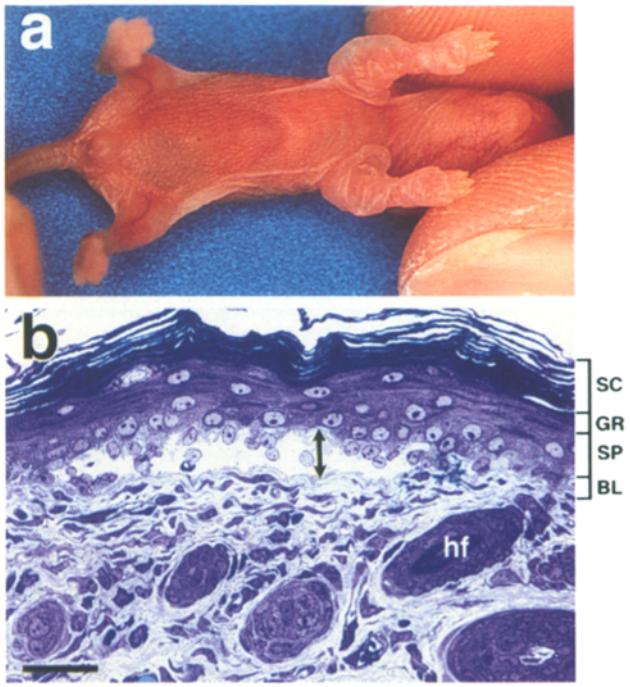


*Figure 3.* Mice homozygous for the targeted K14 allele exhibit gross blistering over their body surface due to cytolysis in the basal layer of the epidermis. (*a*) 2-d-old homozygote (−/−) animal. Note that the front limbs and paws of this mouse are severely blistered. This occurred frequently in these −/− mice in response to mild physical trauma. (*b*) Semithin (0.75 μm) sections of a −/− skin biopsy taken at 2 d of age, embedded in Epon and stained with toluidine blue. Note formation of intrabasal blister, leading to separation of the epidermis from the underlying dermis (double-headed arrow). From bottom to top: *B*, basal layer; *S*, spinous layers; *G*, granular layer; *S*, stratum corneum. *hf*, hair follicle. Bar, 30 μm.

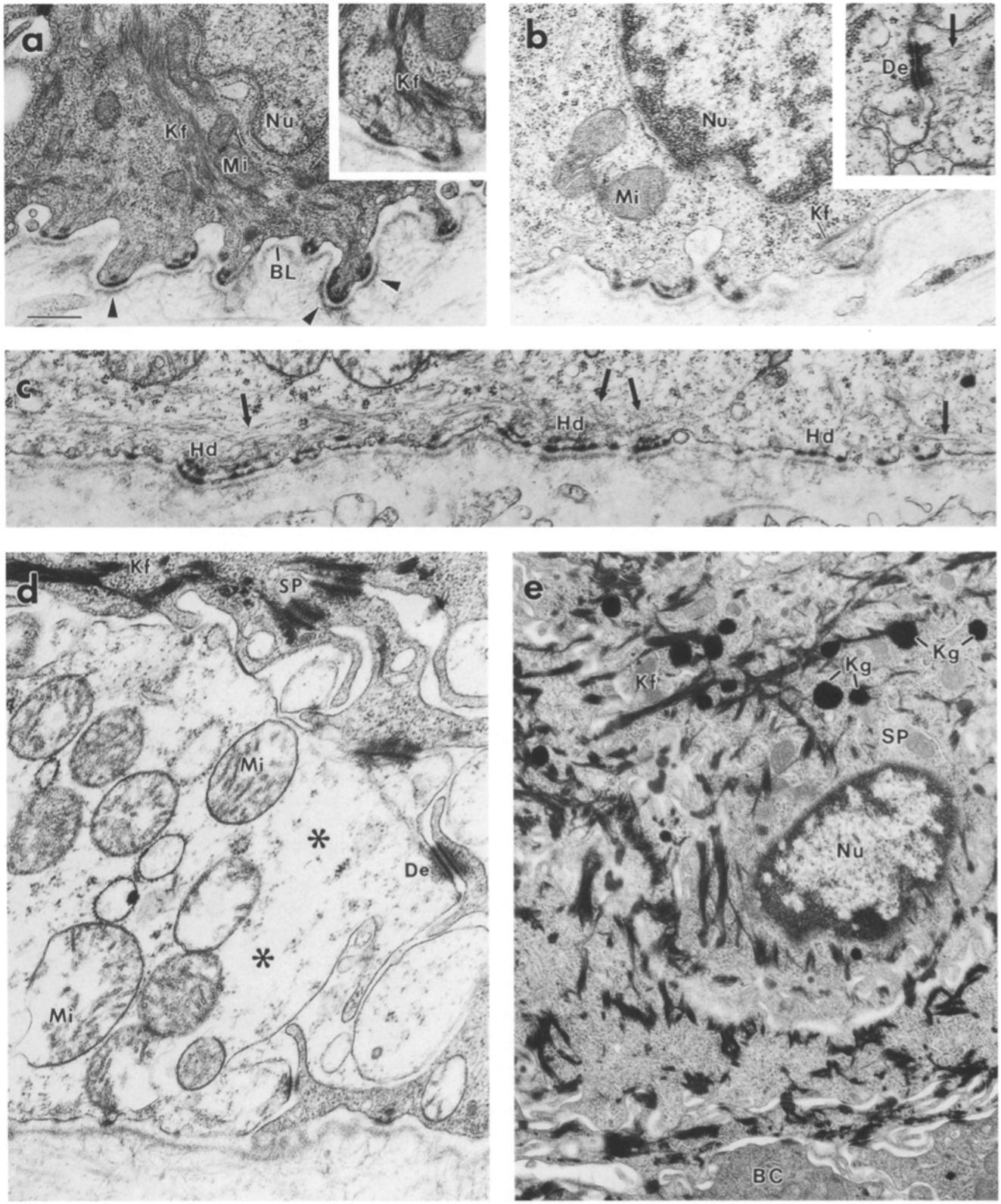


*Figure 4.* The ultrastructure of K14 −/− mouse skin is strikingly similar to that of patients with rare cases of autosomal recessive, severe EBS. Mouse skin samples were taken at 2 d of age, and processed for electron microscopy. (*a*) Basal layer of +/− and (*inset*) +/+ skin. Basal cells show thick bundles of keratin filaments (*Kf*) in cytoplasm. (*Inset*) Keratin filament bundles are attached to hemidesmosomes. *Nu*, nucleus; *BL*, basal lamina; *Mi*, mitochondria; arrowheads, hemidesmosomes. (*b*) Basal layer of −/− mouse skin. Only occasional thin keratin filament bundles (*Kf*) and some sparse keratin filaments are present. (*Inset*) Desmosome (*De*) connecting two basal cells. Arrow denotes presence of a few longer filaments attached to these structures. (*c*) The base of a basal cell from −/− mouse skin. Note presence of an underlying cytoskeleton with filaments (*arrows*) attached to hemidesmosomes (*Hd*). (*d*) Basal and first suprabasal layer of −/− mouse skin. Note extensive basal cell cytolysis (*asterisks*) accompanied by degenerated mitochondria (*Mi*). The suprabasal spinous cell (*SP*) is still intact, with a normal cytoplasm and thick bundles of keratin filaments (*Kf*). (*e*) Suprabasal spinous layers (*SP*) of −/− mouse skin. Note thick bundles of keratin filaments (*Kf*) throughout cytoplasm. In upper layers, Kf bundles are attached to keratohyalin granules (*Kg*). *BC*, basal cell. Bars: (*a–c*, *inset b*) 0.4 μm; (*a, inset*) 0.25 μm; (d) 0.3 μm; (e) 0.75 μm.

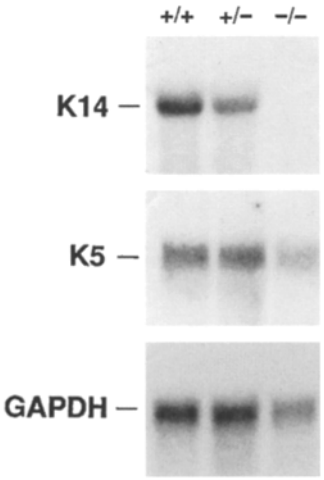


*Figure 5.* Northern blot analyses of skin RNAs from wild-type, heterozygous and homozygous mutant mice. ~20-μg aliquots RNAs isolated from −/−, +/− and −/− mouse skins were resolved by electrophoresis through formaldehyde agarose gels. 18/28S calf liver rRNA and 16/23S E. coli rRNA were run as controls. After briefly staining with EtBr to visualize the rRNA bands, the blots were processed for Northern blot analysis. Blots were hybridized with [$^{32}$P]dCTP radiolabeled DNA probes corresponding to: 13 nucleotides of coding sequence and 125 nucleotides of 3′ noncoding sequence from a mouse K14 cDNA (Knapp et al., 1987); 550 nucleotides from a cloned PCR fragment of mouse K5 exon 1; and 1,600 nucleotides from a glyceraldehyde 3-phosphate dehydrogenase (GAPDH) rat cDNA (internal control; Webster, 1987). To quantitate RNA levels, blots were subjected to phosphoimager analysis (Molecular Dynamics, Menlo Park, CA).

dependently derived K14 +/− ES lines, and therefore, we present the results interchangeably.

### *mK14 Mice Exhibit Gross Blistering Over Their Body Surface*

At birth, homozygous mutants were not distinguishable from heterozygote or wild type littermates. However, within two days after birth, mice became frail and began to show signs of gross blistering over their body surface (Fig. 3 *a*). The degree of skin blistering in newborn animals was significantly more severe than that of the two human EBS patients with K14 premature stop codon mutations (Chan et al., 1994; Rugg et al., 1994). These mice were generally sacrificed within 48 h after birth; however, some survived, and when their first hair coat became plush (~2–4 wk), their body trunk blisters healed, without scarring. Such mice reached adulthood and only showed signs of blistering at skin sites, e.g., ears and paws, which naturally contained sparse hairs and which were subjected to persistent rubbing or scratching. Blistering of adult trunk skin was not as severe in human EBS, presumably due to the protective nature of the hair follicles. This said, the health of adult animals deteriorated over time, and we have not kept mice alive beyond three months.

Light microscopy of neonatal mutant mouse skin revealed blister formation in the basal layer (Fig. 3 *b*). Typical of EBS, initial blister formation was found within the subnuclear cytoplasm of basal cells, and remnants of cytoplasm remained attached to the blister floor. Also typical of EBS, suprabasal layers remained intact and were not distinguishable from control skin.

### *Ultrastructure of Skin of Mutant Mice*

Ultrastructural analyses were performed on skin samples of mice taken at 2–3 d after birth (Fig. 4). Heterozygous +/− skin was indistinguishable from wild-type skin. The cytoplasm from basal epidermal cells from +/+ and +/− mice was rich with bundles of keratin filaments (*a*). Typically, these filament bundles attached to hemidesmosomes (*a*, *inset*) and desmosomes (not shown). In contrast, the most notable feature of the epidermis of K14 −/− mice was the paucity of keratin filament bundles in the basal layer (*b*). A marked absence of keratin filament bundles was also noted previously in basal cells from the two humans homozygous for K14 premature stop codon mutations (Chan et al., 1994; Rugg et al., 1994).

Upon closer inspection, a residual, minor network of wispy filaments was seen attached to hemidesmosomes and desmosomes of the −/− basal cells (*a* and *b*, *inset*, respectively). However, these filaments were sparse and wispy, rather than bundled. These structures were also noted in the putative K14 null patients; however, their identity was left undetermined, and their origin was a matter of speculation and controversy (Chan et al., 1994; Rugg et al., 1994). Finally, the suprabasal layers of skin of −/− mice were indistinguishable from normal. Keratin filament

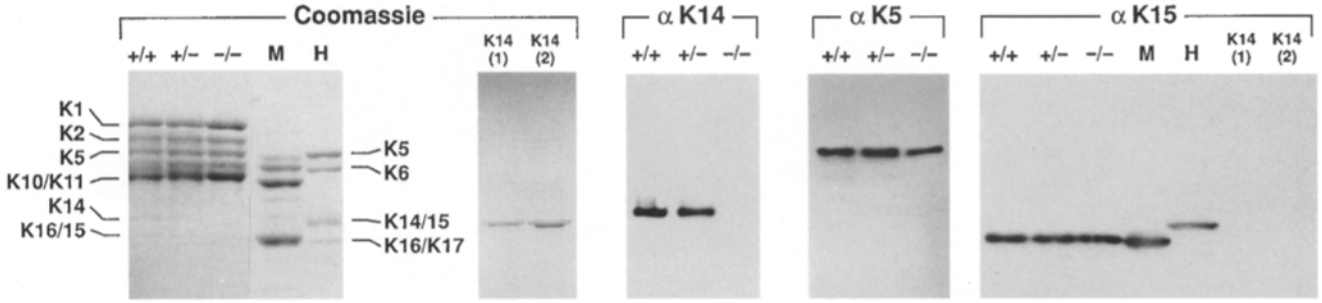


*Figure 6.* Immunoblot analyses of skin IF proteins from wild-type, heterozygous, and homozygous mutant mice. IF proteins were extracted from backskins of 2-d-old −/−, +/−, and +/+ mice, and resolved by electrophoresis through 8.5% SDS–polyacrylamide gels (Wu et al., 1982). Gels were either subjected to Coomassie blue staining or immunoblot analyses. Immunoblots were developed using the antibodies K14 (1:10,000 dilution), K5 (1:40,000 dilution), and K15 (1:5,000 dilution), followed by horseradish peroxidase secondary antibodies and processing with a chemiluminescent substrate (ECL method; Amersham Corp.). Proteins were from: M, IF extract from wild-type mouse tongue (rich in mouse K6 and K16); H, IF extract from cultured human keratinocytes (rich in K5, K6, K14, K16 and K17); K14 (1) and (2), purified recombinant human K14 protein (1 and 2 μg, respectively). Keratins are identified according to the nomenclature of Moll et al. (1982*a*), with the mobility of mouse keratins at left and human keratins at right. Note that human K14 runs at 50 kD and mouse K14 runs at 52 kD. Note also that human K15 runs at 50 kD and mouse K15 runs at 48 kD.

bundles were typical in appearance and number to normal suprabasal filaments (Fig. 4, *d* and *e*).

### *Absence of K14 mRNA and Protein in Skin of −/− Mutant Mice*

To assess whether the targeted homologous recombination resulted in ablation of K14 mRNA, we conducted Northern blot analysis on total RNAs extracted from mouse skins (Fig. 5). K14 mRNA levels correlated well with the number of wild-type K14 alleles present in the genomes of these animals. In contrast, K5 mRNA levels were largely unaffected, when differences in loadings were normalized.

In our initial construct, we had placed a human vimentin cDNA just downstream from the K14 promoter. We probed our blots with a full-length human vimentin cDNA, but no mRNA was detected, indicating that the endogenous K14 promoter was not competent to drive its expression (data not shown). We also followed this up at the level of immunoblot analysis, and verified that no vimentin protein was produced from our knockout construct (not shown). Thus, this construct was a knockout rather than a replacement vector. We will deal with issues of replacement in the future.

To examine keratin protein profiles, we conducted SDS–polyacrylamide gel and immunoblot analyses on IF extracts from skins of +/+, +/− and −/− mice (Fig. 6). Coomassie blue staining revealed the complex pattern of keratins typical of mouse epidermis (Fig. 6, *left*; Moll et al., 1982*a*,*b*; Schweizer et al., 1984). As expected, in total IF extracts, differentiation-specific keratins were far more abundant than basal keratins, which were very faint on these gels. Although there were mouse counterparts to the various human skin keratins, some of them, e.g., K14 and K15, migrated differently.

Immunoblot analysis with a monospecific anti-K14 (αK14) peptide antiserum revealed clearly that the mouse K14 band (52 kD) was missing in the −/− IF sample (Fig. 6). The K14 protein level in the +/− sample did not reflect the reduced K14 mRNA level, although this may be due to a lesser sensitivity of protein analysis rather than a reflection of posttranslational control in keratin regulation.

### *K15 Is a Natural Partner for K5 and These Keratins Constitute a Residual Keratin Network in K14 −/− Basal Epidermal Cells*

The anti-K5 (αK5) immunoblot of these proteins confirmed the existence of K5 in all three samples (Fig. 6). It was surprising that the levels of K5 were appreciable in the −/− mouse sample, since the stability of a type II keratin is known to be dependent upon its partner (Kulesh and Oshima, 1988; Lersch et al., 1989). In previous studies on the putative K14 null EBS patients, several mechanisms were proposed to account for the stabilization of K5 (Chan et al., 1994; Rugg et al., 1994). In one study, it was suggested that another type I keratin might complex with K5 (Chan et al., 1994).

If some K5 expression continues after K10 induction, some stabilization of K5 would be conferred by differentiation-specific type I keratins. While αK5 immunostaining is restricted to the basal layer, it is known that K5 and K14 protein persist in suprabasal layers (Fuchs and Green, 1980). A second basal type I keratin could provide additional stability, should one exist. K15, a minor component of epidermis, is one candidate for a second basal type I keratin. To examine this possibility, we raised a rabbit polyclonal antiserum monospecific for a peptide corresponding to the 12 amino acids at the carboxy terminus of K15. This antisera detected a mouse protein of 48 kD and a human protein of 50 kD (Fig. 6). The αK15 antibody did not cross-react with recombinant human K14 protein, which also migrates as a 50-kD protein on SDS–polyacrylamide gels. These data verified the specificity of the antisera and established that K15 is expressed in mouse epidermis. Hybridization was comparable in all three samples, suggesting that K15 levels were not appreciably affected by K14 ablation.

To assess the location of K14, K5 and K15 in the skin of our animals, we conducted immunohistochemistry (Fig. 7). As expected, the αK14 antiserum labeled the basal layer of epidermis and the ORS of hair follicles of +/+ and +/− skin (Fig. 7 *a*). This antiserum showed no labeling of −/− skin (Fig. 7 *b*), consistent with our immunoblot analyses showing the complete absence of K14 in mutant mice. The αK5 antiserum labeled the basal layer of the epidermis and the ORS from all skin samples (Fig. 7, *c* and *d*).

Our new αK15 antiserum also labeled the basal layer of epidermis and the ORS from all skin samples (Fig. 7, *e* and *f*). These data provided the first documentation of K15 localization and provided compelling evidence that K15 is indeed a partner type I keratin for K5 protein in the −/− mice. Finally, αK6 labeled the ORS of all samples, consistent with its natural location (Fig. 7, *g* and *h*). In contrast to a classical wound-healing response, K6 (and presumably its partner K16) did not seem to be induced in the epidermis of mice ablated for K14.

To investigate whether K15 is a part of the normal keratin network of basal cells, and whether this protein can assemble into bona fide keratin filaments, we conducted immunoelectron microscopy on skin and tongue, two tissues which in wild-type mice, have extensive basal keratin networks (Fig. 8). Each of these three antibodies heavily labeled the dense keratin filament bundles of control basal cells (Fig. 8, *a*–*c*′). The αK15 labeling was highly specific, and clearly showed that this keratin is a component of the normal keratin network of basal cells (Fig. 8, *c* and *c*′).

To assess whether K5 and K15 are the components of the residual keratin network in K14 −/− basal cells, we conducted additional immunolabelings. αK5 antibodies strongly labeled filaments found at the cell periphery and in the cytoplasm of −/− epidermal and tongue basal cells (Fig. 8, *d* and *e*, respectively). αK15 antibodies also showed strong labeling of these filaments (Fig. 8 *f*). αK15 (and αK5) labeling was also detected in the vicinity of hemidesmosomes and desmosomes of −/− basal cells (Fig. 8, *g*–*i*). In cases where desmosomes connected two basal cells, both sides of the plaque labeled with these antibodies (Fig. 8 *h*). In cases where desmosomes connected a basal and suprabasal cell, only the basal side of the plaque exhibited labeling (Fig. 8 *i*). These findings established the specificity of the antibodies and unequivocally demonstrated that K14 −/− basal cells produce a residual IF network of K5 and K15.

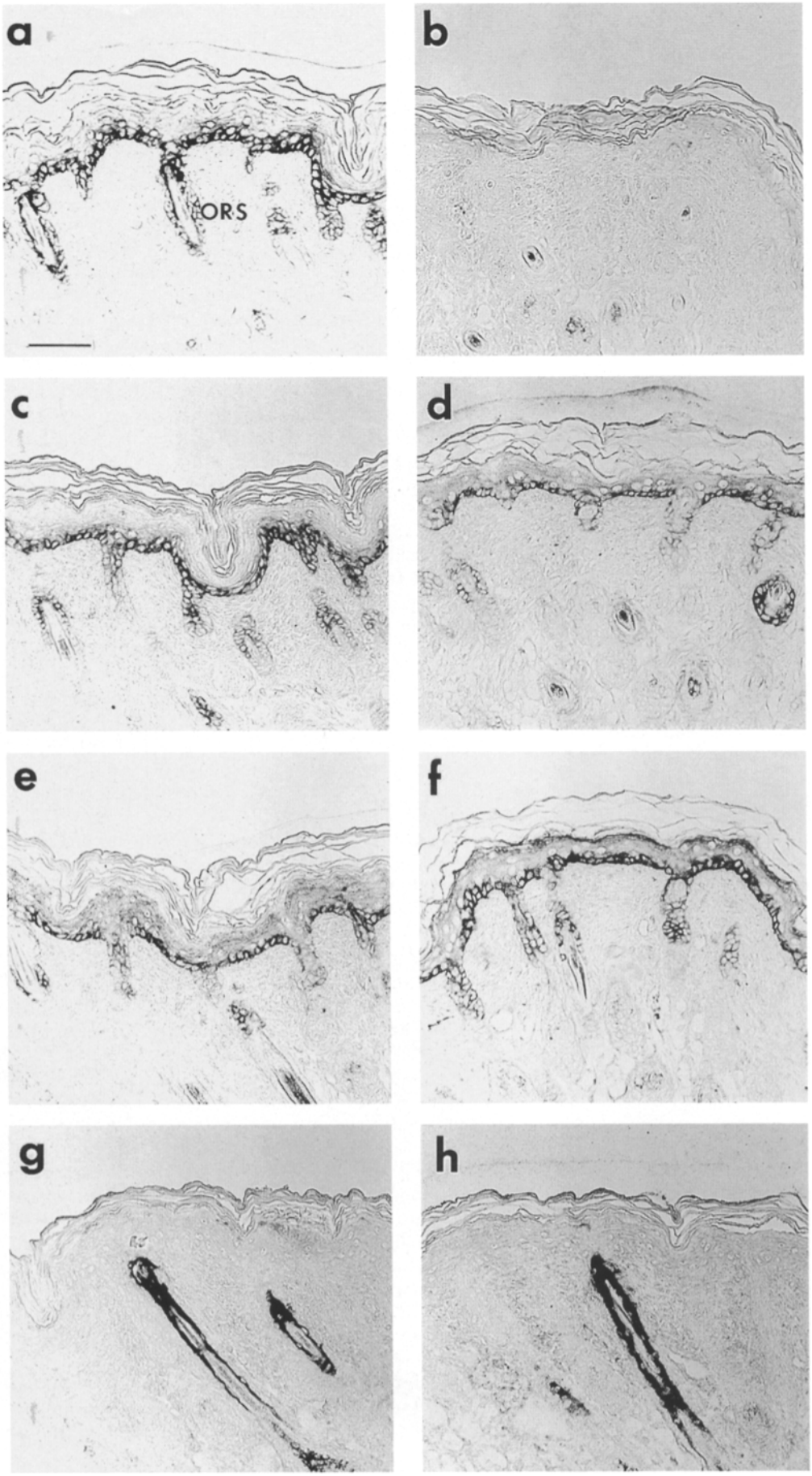


*Figure 7.* Immunohistochemistry of mutant mouse skin. Sections of backskins of two day old −/− and +/− mice were subjected to immunohistochemistry, using immunogold enhancement (Kopan and Fuchs, 1989). *a*, *c*, *e*, and *g* are from +/− skin; *b*, *d*, *f*, and *h* are from −/− skin. (*a* and *b*) αK14; (*c* and *d*) αK5; (*e* and *f*) αK15; (*g* and *h*) αK6. ORS denotes outer root sheath of hair follicle. Bar, 50 μm.

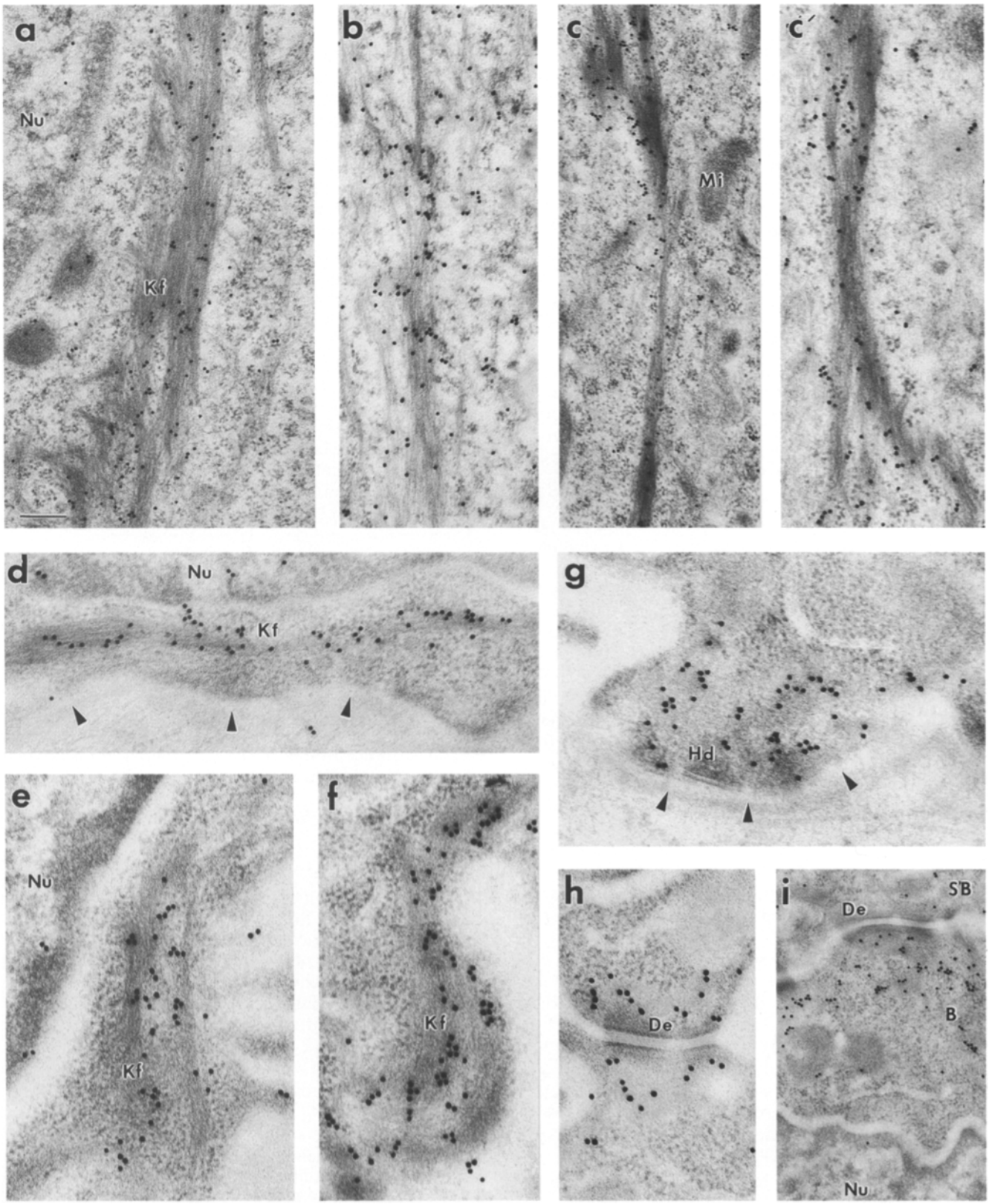


*Figure 8.* Immunoelectron microscopy of control and mutant mouse epithelium. Samples of 2-d-old +/− and −/− skin and tongue samples were embedded in Unicryl and subjected to 30 nm gold labeling. (*a–c'*) Wild-type basal epidermal cells from tail skin labeled with (*a*) αK14, (*b*) αK5, (*c* and *c'*) αK15. (*d*) αK5 of −/− basal cell from tail skin. (*e*) αK5 of −/− basal cell from tongue. (*f–i*) αK15 of −/− basal cells from tongue. (*h*) shows example of desmosome between two adjacent basal cells; (*i*) shows example of desmosome between a basal (*B*) and suprabasal (*SB*) cell. *Nu*, nucleus; *Mi*, mitochondria; *De*, desmosome; *Hd*, hemidesmosome; *Kf*, keratin filament bundles; arrowheads, basal lamina. Bars: (*a–c'*) 0.3 μm; (*d–h*) 0.2 μm; (*i*) 0.4 μm.

The IFs composed of K14, K15, and K5 were more thickly bundled than those composed only of K5 and K15. Later, we show that this is likely to be a feature of K15 and K5 filament properties rather than merely the sparse density of these filaments in −/− skin. Irrespective of this issue, the studies on skin indicated that the K5-K15 network of filaments was not sufficient to impart to these cells the mechanical strength necessary to withstand physical trauma.

### *The Effects of K14 Ablation on Other Stratified Squamous Epithelia*

K5 and K14 are expressed in the basal layer of all stratified squamous epithelia, and have been considered to be the pair of keratins that typify these tissues (Moll et al., 1982*a*; Nelson and Sun, 1983). Thus, we anticipated that there might be abnormalities in the architecture of other stratified K14 −/− tissues. Such studies were not possible for the rare human recessive EBS cases (Chan et al., 1994; Rugg et al., 1994), and given the weakness of the basal keratin promoters in many internal stratified tissues (Byrne and Fuchs, 1993; A. Leask, S. Zinkel and E. Fuchs, unpublished observation), definitive answers were not possible from analyses of transgenic mice expressing dominant negative K14 mutants (Vassar et al., 1991; Coulombe et al., 1991*b*).

We examined the ultrastructure of cornea, dorsal and ventral tongue, forestomach and esophagus from neonatal −/− tissues. Only two of these tissues showed major and consistent signs of basal cell cytolysis: (*a*) epidermis of skin in areas where a thick protective hair coat was not present (Fig. 4 *d*), and (*b*) cornea (Fig. 9 *a*). The cytolysis in corneal epithelium appeared to give rise to a thinner tissue, as judged by comparison with epithelial samples taken from similar locations of control corneas (Fig. 9, *a* and *b*, respectively). Corneal basal cells differed from basal epidermal cells in their shape. The flattened, rather than columnar, nature of corneal cells presumably stems from the fact that corneal basal cells arise from centripetal migration of stem cells located in the limbus (Schermer et al., 1986). When the migrating cells undergo extensive cytolysis as they do in the K14 −/− mice, this reduces the population of migrating cells, likely resulting in a thinner epithelium.

A second difference between corneal and epidermal basal cells was in the density of their keratin filament networks. In contrast to normal basal epidermal cells, which were rich with bundles of keratin filaments (Fig. 4 *a*), normal corneal basal cells had only a very sparse keratin network, which was difficult to visualize even at high magnification (Fig. 9, *b* and *inset*). Surprisingly, this sparse network of filaments in normal corneal basal cells resembled more closely the mutant epidermal basal cell than a normal epidermal basal cell. Despite this similarity, normal corneal basal cells did not display the fragility of mutant epidermal basal cells. From this comparison, we concluded that the fragility of a basal stratified squamous epithelial cell cannot be measured simply by the density of its keratin network.

Another interesting complexity surfaced when we examined the basal layer of the dorsal surface of the tongue of mutant and control animals (Fig. 9, *c* and *d*, respectively). Ultrastructurally, the wild-type basal cells of tongue and epidermis were similar (compare Fig. 9 *d* with 4 *a*). These cells were columnar in shape and displayed an array of thick keratin filament bundles in their cytoplasm. The −/− tongue basal cells resembled the −/− epidermal basal cells, except for a somewhat greater amount of residual keratin filaments in their cytoplasm (compare Fig. 9 *c* with 4 *b*). Overall, however, the thick dense bundles of keratin filaments, typical of both tongue and epidermal basal cells, were missing, and most of the residual filaments were attached to desmosomes and hemidesmosomes (Fig. 9 *c*). Despite these similarities, we did not detect signs of gross cytolysis in the tongues of the −/− mice that we examined. Assuming that the small differences in keratin filament numbers do not account for this difference, it seems most likely that tongue basal cells are subjected to less trauma than epidermis, and hence undergo less cytolysis. An additional feature which might provide protection is the undulation of the tongue epithelium into the underlying mesenchyme. Such anchorage might protect in a manner similar to that of hair follicles.

A final surprise came in examining the innermost layers of the −/− neonatal forestomach and esophagus (Fig. 9, *e* and *f*, respectively). Although the keratin filaments of −/− esophageal basal cells were not densely bundled (Fig. 9 *f*), they were not significantly different in size or number than the keratin filaments in the control. This was also the case for the forestomach (Fig. 9 *e*). Furthermore, the −/− basal cells of forestomach and esophagus showed no signs of cell cytolysis. While lack of cytolysis in esophagus had also been noted in dominant negative K14 mutant mice (Vassar et al., 1991; Coulombe et al., 1991*b*), it had been assumed that this was due to a combination of the weak promoter activity driving the transgene and to the suspicion that internal epithelia were not under as much physical stress as surface tissues. These new findings indicate that there may be a different underlying explanation.

### *Analysis of K15 in Stratified Squamous Epithelia*

All stratified squamous epithelia that we examined from our K14 −/− neonatal mice displayed some keratin filaments in their basal cells. Since K5 and K15 are constituents of the residual network in basal epidermal cells, we wondered whether K5 and K15 might also be components of the residual networks of other basal cells. To test this possibility, we conducted immunohistochemistry on stratified squamous epithelia from control and −/− mice (Fig. 10). In all cases, the data were indistinguishable for control and −/− samples, and therefore only the data for the −/− mouse tissues are shown.

Both tongue and forestomach showed basal layer staining with αK5 and αK15 (*a* and *b* tongue; *c* and *d* forestomach; αK5 left; αK15 right). Esophagus showed αK5 and αK15 staining throughout all layers (*e* and *f*, respectively). In all cases, αK14 followed similar patterns when control tissues were examined, and showed no staining of −/− tissues (not shown). Collectively, these data indicated that basal keratin networks of many stratified squamous epithelia contained not only K5 and K14, but also K15.

The wide variation in density of keratin filaments in basal cells of different −/− neonatal stratified squamous epithelia led us to wonder whether the ratio of K14 and K15 might differ among these tissues. To begin to explore

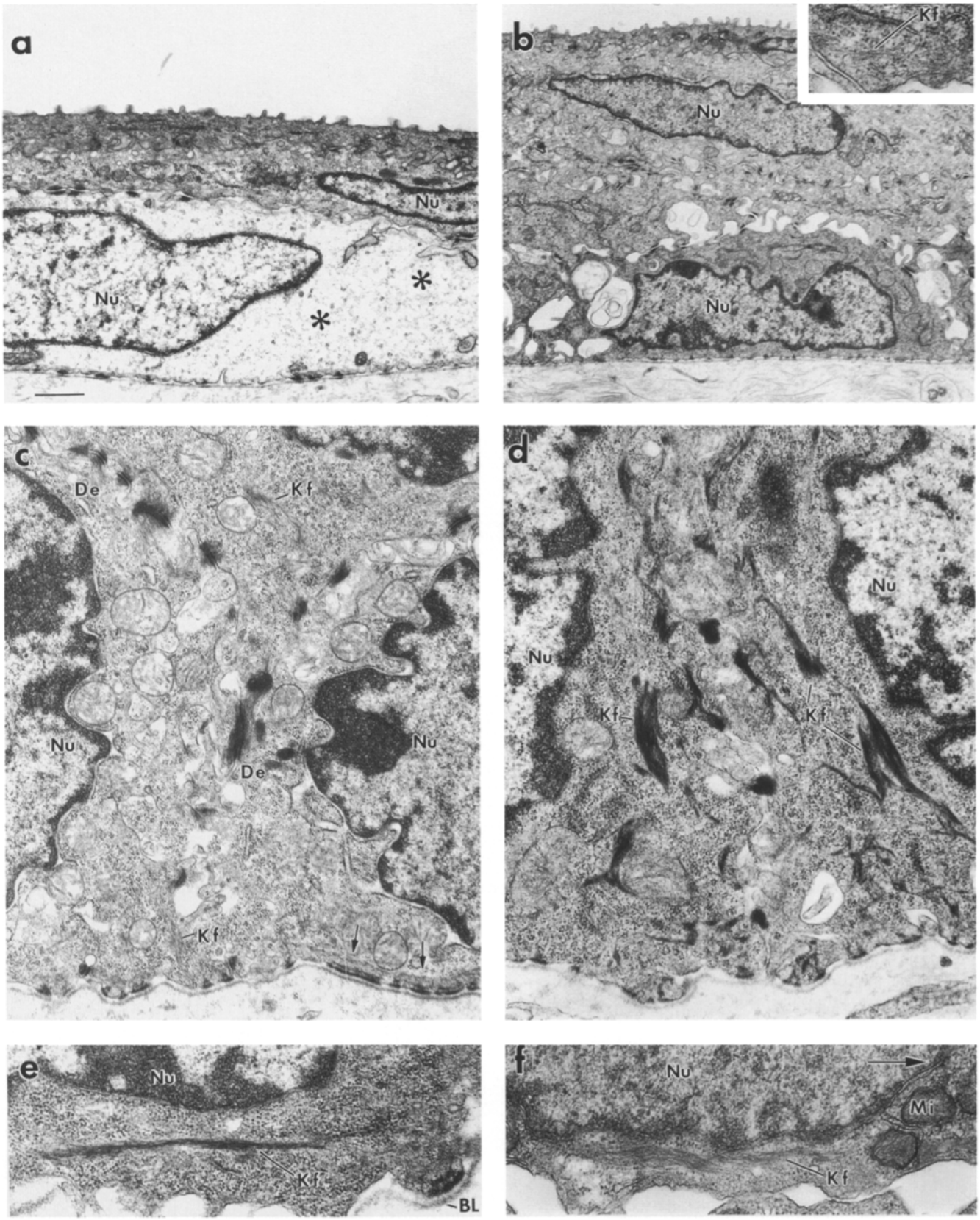


*Figure 9.* Ultrastructure of other stratified squamous epithelia of neonatal mutant mice. Tissues from 2-d-old −/− and +/− mice were fixed and processed for electron microscopy. Sections shown are from: (*a*) cornea of −/− mouse. Asterisks denote cytolysis. (*b*) cornea of +/− mouse. Inset, thin and sparse keratin filament bundles (*Kf*) typical of normal corneal basal cells. (*c*) Basal cells of dorsal portion of a −/− tongue. Note presence of small keratin filament bundles, which were more prevalent than those of −/− epidermis. Note also the denser filaments surrounding desmosomes (*De*) and hemidesmosomes (*arrows*). (*d*) Basal cells in dorsal portion of a +/− tongue. Note thick keratin filament bundles (*Kf*) typical of wild-type basal cells of both tongue and epidermis. Frames *e* and *f*. Basal cells from a −/− forestomach (*e*) and esophagus (*f*). Note long and relatively thin keratin filament bundles (*Kf*), typical of wild-type basal cells from these tissues. In fact, very little difference was detected between the wild-type and −/− basal cells from these two tissues. Arrow in *f* denotes direction of basement membrane. *Nu*, nuclei; *BL*, basal lamina; *Mi*, mitochondria. Bars: (*a*) 0.8 μm; (*b*) 1.3 μm; (*b*, *inset*) 0.35 μm; (*c*) 0.55 μm; (*d*) 0.45 μm; (*e* and *f*) 0.4 μm.

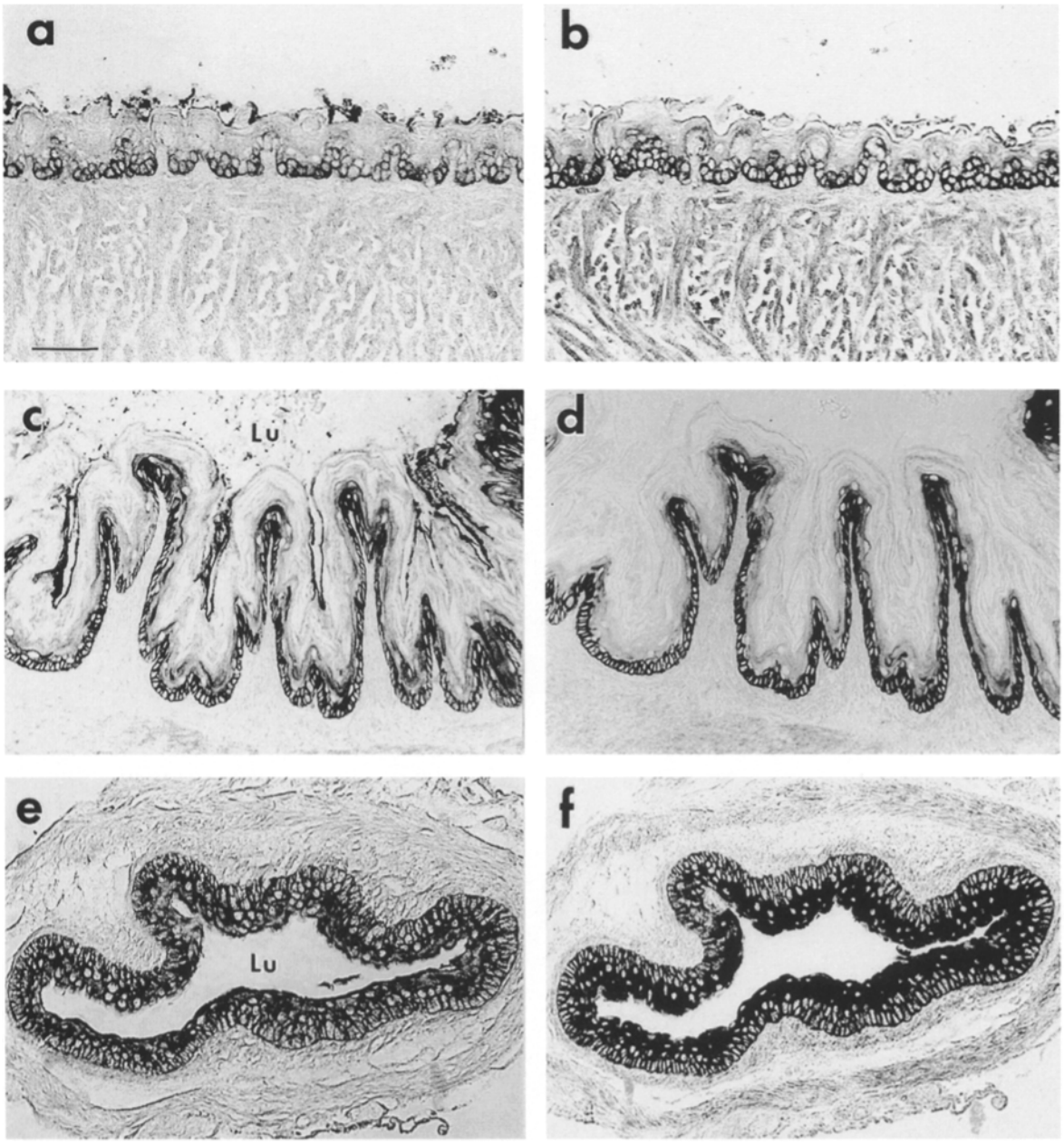


*Figure 10.* Immunohistochemistry of stratified squamous epithelia of mutant mouse. Sections of tissues of 2-d-old −/− mice were subjected to immunohistochemistry, using immunogold enhancement (Kopan and Fuchs, 1989). (*a* and *b*) αK5 and αK15 labeling of dorsal region of tongue; (*c* and *d*) αK5 and αK15 labeling of forestomach; (*e* and *f*) αK5 and αK15 labeling of esophagus. *Lu*, lumen. Bar, 50 μm.

this possibility, we used immunoblot analysis of IF proteins to compare the signals of αK14 and αK15 in a tissue, relative to a constant signal of αK5 (Fig. 11). Interestingly, the levels of K15 relative to K5 did not seem to change significantly in the absence or presence of K14. This finding is difficult to reconcile on the basis of either K15- or K10-induced stabilization of K5. It suggests that another mechanism must also contribute to the maintenance of K5 levels when K14 is absent.

The relative amounts of K14 and K15 varied dramatically among tissues. IF extracts of skin and thymus showed strong αK14 labeling but very low levels of αK15 labeling. While this method did not allow us to determine absolute levels of K14 and K15, the immunoblot data were consistent with the Coomassie blue stained profile of these proteins (not shown; see also Moll et al., 1982*b*; Chan et al., 1994), indicating that there is significantly more K14 than K15 in neonatal skin.

While the αK14 signal was very strong in tongue, the αK15 signal was stronger in tongue than in skin (Fig. 11). This provided an explanation for why the residual keratin network in basal tongue cells was higher than that of basal epidermal cells in the −/− mice. Interestingly and opposite to skin and tongue, IF extracts from neonatal esophagus showed a much stronger signal for αK15 than for αK14 (Fig. 11). When taken together with our ultrastructural

data on this tissue, this provides an explanation for why ablation of K14 did not result in any significant decline in filament numbers or architecture in this tissue. Thus, at the extreme ends of the scale, a tissue such as epidermis, with a high αK14/αK15 ratio showed marked cell fragility and cytolysis when K14 was ablated, while a tissue such as esophagus, with a high αK15/αK14 ratio showed little or no effect.

Forestomach and cornea gave results intermediate between those of skin/tongue and esophagus (Fig. 11). Thus, αK14 and αK15 staining was comparable in these extracts. It is curious that despite the similarities in K14/K15 ratios, corneal basal cells responded to the loss of K14 by a marked increase in cell fragility, whereas forestomach epithelium showed no difference from wild-type cells. At the moment, we cannot explain these results. It could be that there is a novel type I keratin in forestomach that contributes to the overall network of its basal cells, and which provides extra mechanical integrity when K14 is ablated. Alternatively, it could be that the physical properties of these two cell types are inherently different, an indication of which stems from the shape of their basal cells and the levels of their keratin filaments.

Additional experiments will be necessary to uncover all of the complexities of different stratified squamous epithelia and their varied responses to K14 ablation. However, we found no indications from our Coomassie blue stained gels to suggest that there might be a new keratin induced in any of the stratified squamous epithelial tissues we examined (not shown). These data further underscore the failure of basal cells to adjust their expression of keratins when K14 is lost. Thus, in the future, explorations into these differences will focus more on the nature of physiological differences between various epithelia, and on examining the consequences of ablating K15.

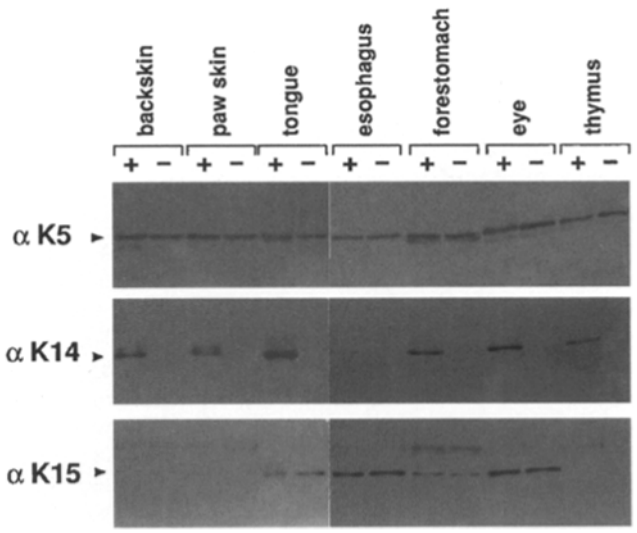


*Figure 11.* Immunoblot analyses of IF proteins from stratified squamous epithelia of homozygous mutant mice and control littermates. IF proteins from various −/− (−) and +/− (+) tissues known to express K14 in their wild-type state were resolved by electrophoresis through 8.5% SDS–polyacrylamide gels (Wu et al., 1982). Loadings were adjusted such that the levels of K5 in each preparation were approximately the same. Gels were either subjected to Coomassie blue staining (not shown) or immunoblot analyses. Immunoblots were processed using αK5 (1:600 dilution), αK14 (1:900 dilution), or αK15 (1:900 dilution) primary antibodies, and alkaline phosphatase-conjugated secondary antibodies. Blots were then developed with a color enhancement substrate (Bio Rad Labs). The appropriate keratin bands identified by each antiserum are denoted by the arrowheads. Note: the faint band of higher molecular mass visible on the αK15 immunoblot shown was an artifact, and typically disappeared upon longer washings of blots (see Fig. 6).

### *The Ratio of K15/K14 in Esophageal Basal Cells Changes with Age*

We were puzzled by the deterioration in health of older −/− animals, despite the seeming improvement over most of the body surface. Animals continued to have blisters in areas that were not protected by a thick covering of body hairs, and this was most pronounced on the ears, face and neck. However, dissection of an adult animal revealed an additional enigma, and a likely explanation for its poor health. A number of internal stratified epithelia, including esophagus, vagina and trachea, were visibly affected. Vaginal epithelium was blistered, and when esophagus and trachea were dissected, they tended to break and disintegrate easily. This was surprising, since we had observed no abnormalities in internal tissues of the neonatal −/− mice.

Ultrastructural analysis of esophageal tissue from adult −/− and control animals revealed a significant difference between the number of keratin filaments in both basal and suprabasal layers (Fig. 12, *a* and *b*). Moreover, the −/− cells had a network of dispersed filaments, more similar to that of the esophagus of neonatal control mice, whereas the esophageal cells from the control adult had a network of bundled keratin filaments, more similar to that of epidermis or tongue. While we did not detect cytolysis in the specific regions of −/− tissues examined, the brittleness of these tissues suggested that mechanical stress could compromise their functioning in the adult.

The ultrastructural differences seen in adult esophageal epithelia were in striking contrast to neonatal esophageal tissues, which showed no major differences between −/− and control animals. The apparent fragility of esophagus and certain other stratified tissues suggested that the relative K15 and K14 levels in these cells might be changing during postnatal development. To test this possibility, we compared these profiles by polyacrylamide gel electrophoresis and immunoblot analysis. As shown in Fig. 12 *c*, K15 was a major type I keratin of the neonatal esophageal tissue sample and was significantly more abundant than K14. In contrast, K14 became abundant in the adult sample. Collectively, these data demonstrated that the contribution of K14 to adult esophageal tissue was significantly greater than to its neonatal counterpart, a feature likely to underlie the aberrances that develop in this tissue during postnatal development of −/− mice.

## *Discussion*

### *The K14 Knockout in Mice as Compared to Human*

Our knockout mice provide the first case where comparable K14 mutations have been described in human EBS pa-

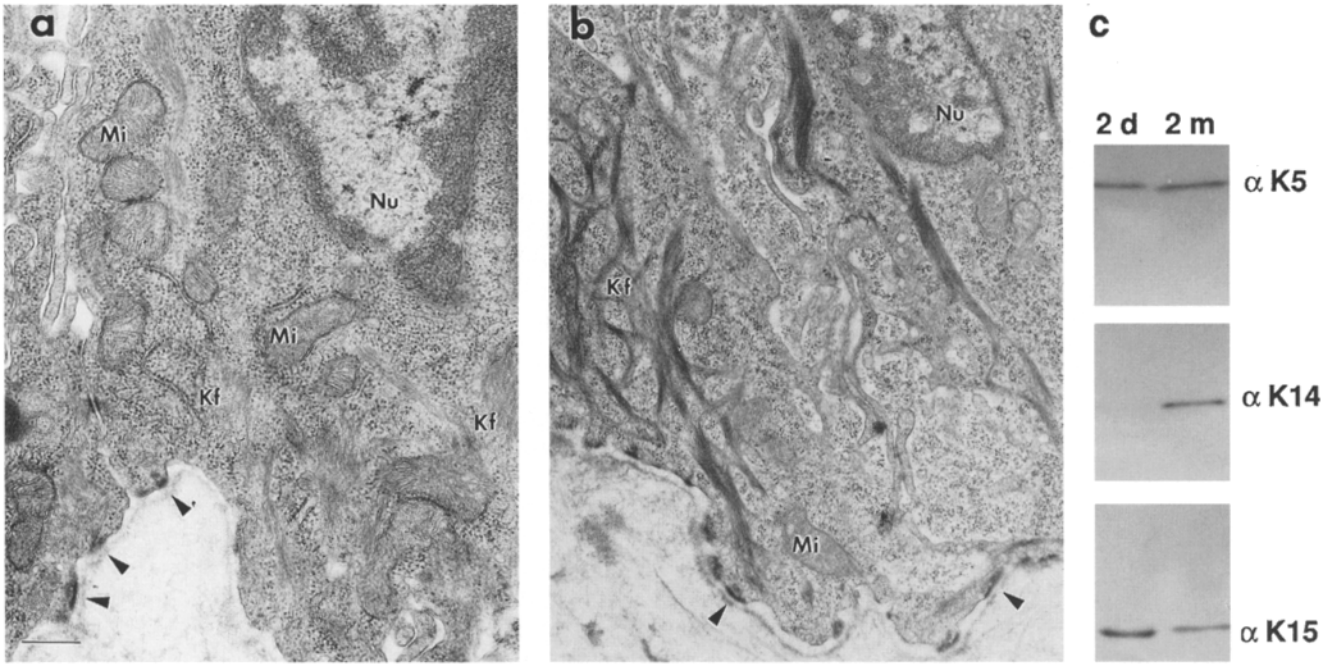


*Figure 12.* Ultrastructure and basal IF proteins of esophagus of adult mutant mice. (*a* and *b*) Esophageal tissues from 2-mo-old −/− and +/− mice were fixed and processed for electron microscopy. Sections shown are from: (*a*) −/− mouse and (*b*) +/− mouse. Note marked differences in the number and arrangement of keratin filaments (*Kf*) in these two samples. *Nu*, nuclei; *Mi*, mitochondria; arrowheads, basal lamina/hemidesmosomes. (*c*). IF proteins were extracted from esophageal tissues of 2-d-old and 2-mo-old wild-type mice. Proteins were resolved by SDS–polyacrylamide gel electrophoresis and subjected to immunoblot analysis to identify keratin proteins. Note: Coomassie blue-stained gels of these samples revealed that the differences in absolute levels of K14 and K15 in these samples are similar to those that are reflected by αK14 and αK15 labeling. Bar, 0.45 μm.

tients and in mice. The mice displayed severe blistering over their front limbs, a feature which would be classified as Dowling-Meara in humans. In contrast, both humans were clinically diagnosed as Koebner, a less severe form of the disease (Chan et al., 1994; Rugg et al., 1994). It is possible that genetic background may influence severity, and further studies will be necessary to assess whether the level of blistering varies with mouse strain and/or human genetic background.

The severity of blistering in K14 −/− mouse skin lessened in regions which became covered with a thick hair coat, supporting the notion that blistering is associated with mechanical trauma. In humans, skin blistering also improves with age. While the hair coats of humans and mice are very different, anchorage becomes deeper as the follicles mature, and this feature may protect EBS epidermis in adult humans as well as in mice.

The deterioration of the overall health of adult K14 −/− mice was striking. Since the two human K14 knockout cases are still in their youth, it will not be known for some time whether the deterioration seen in K14 −/− mice will also occur in these patients. In autosomal dominant EBS, the skin blistering of patients clearly improves with age. It has not been reported that the oral or internal lesions found in severe cases worsen with age, although this may be useful to examine in the future. On the other hand, it is possible that species-specific differences may prevent brittleness of internal stratified tissues in adult K14 −/− humans.

### *A New Basal Keratin in the Picture: New Insights into Disease and Keratin Regulation*

Our studies indicate clearly that in contrast to previous assumptions, K5 has two natural partners instead of one. One reason that K15 has been largely overlooked is that its size in humans is 50 kD, i.e., the same as that of K14. In the absence of a monospecific antiserum for K15, previous examination of this protein has been restricted to analysis by two dimensional gel electrophoresis. The lack of interest in K15 also rests in prior assumptions that it was a minor cytoskeletal component of stratified tissues (Moll et al., 1982*a*,*b*; Nelson and Sun, 1983). This misconception seems to have arisen from extrapolation of studies on skin, where K15 is a minor component (Moll et al., 1982*b*), and from studies on adult internal stratified tissues, where the levels of K14 are higher than in the corresponding neonatal tissues (Moll et al., 1982*a*; Leube et al., 1988). When taken together with its unusual expression pattern, our studies on K15 suggest that in contrast to K14 mutations which give rise to EBS, K15 mutations might give rise to patients with perhaps mild symptoms of EBS in the skin, but more severe symptoms in internal stratified squamous epithelia. Future studies will address this possibility.

Cell culture studies have indicated that K5 is degraded in the absence of K14 (Kulesh and Oshima, 1988; Lersch et al., 1989; Chan et al., 1994). In epidermis, however, the reduction in K5 protein was not as dramatic as might have been expected based on the paucity of filaments in the basal layer of K14 −/− epidermis (Rugg et al., 1994;

present study). While we documented that K15 and K5 constitute the residual keratin network, the K5 levels seem too high to be complexed solely with K15. Some of the excess K5 seen in vivo may also be a reflection of stabilization provided by K10 in the first suprabasal layer. Such a phenomenon could occur if there were either a relatively short delay or perhaps even a short overlap between cessation of K5 synthesis and induction of K10 synthesis. However, these arguments still do not seem to account fully for the maintenance of K5. Rugg et al. (1994) suggested that excess K5 might be stabilized by association with the membrane, but we did not see any preferential localization of αK5 versus αK15 in these areas. This dilemma, presently unsolved, merits further investigation in the future. Finally, it was interesting that the overall expression programs of all of the keratins seemed to be independent of K14 expression, and that the absence of K14 did not appear to stimulate any compensatory mechanisms in any of the stratified squamous epithelia tested.

### *The Consequences of K14 Ablation and Possible Differences in K5-K15 Versus K5-K14 Networks*

The K5-K15 filaments observed in the skin of homozygous K14 null mice differed from the bundles of K5-K14 keratin filaments characteristic of control basal cells. Now that we have found that K15 is a component of the normal keratin network in epidermal basal cells, it is likely that these residual filaments in the mutant cells are bona fide IFs. Support for this notion came from examining tissues such as neonatal esophagus, which had much higher levels of K15 than K14, and which had IF networks that appeared unchanged as a consequence of K14 ablation. The difference in IF bundling seems to reflect differences in the physical properties of K5-K15 versus K5-K14 filaments, as judged by the parallel increases in IF bundling and K14 expression in esophageal basal cells as they developed postnatally. This said, these differences could also arise from changes in auxiliary IF-associated proteins that might have also changed with development.

Another interesting issue is whether the mechanical integrity of a K5-K15 network is comparable to one which contains K5, K14 and K15. While this issue has not been unequivocally resolved, there are some indications to suggest that it may not be the case. Thus, the adult −/− esophagus was clearly brittle, even though it had an extensive network of disperse K5-K15 filaments. Why aren't basal cells of control neonatal esophagus also fragile, since they have an even sparser network of K5-K15 filaments than −/− basal cells of adult esophagus? This could be due to differences in mechanical strength requirements: neonatal mice have a liquid diet, whereas adults eat whole food. If correct, this would explain why the levels of K14, and the overall density of keratin filaments, increases during postnatal development in esophagus. Future studies will address this issue in greater detail.

Our studies reveal that it is not simply the overall density of a keratin filament network that determines the mechanical integrity of a basal cell. Why don't basal cells from tissues such as cornea need as extensive a keratin network as those from tissues such as the epidermis? An answer to this question comes from considering what happens to basal epidermal cells of EBS patients and/or mice during wound-healing (Anton-Lamprecht, 1983; Coulombe et al., 1991*b*). In this case, cells become temporarily resistant to lysis, a period which lasts while the columnar basal cells flatten out and migrate into the wound. Hence, cells that have a flattened shape may not be as dependent upon an extensive keratin network as those that are columnar in nature. We do not yet understand why flattened corneal basal cells become fragile when their K14 is ablated, whereas flattened epidermal basal cells at the site of a wound do not. As suggested above, it may be that factors such as the specific keratins composing the network may be central to cytoskeletal architecture and design.

Finally, for all stratified squamous epithelia examined, the terminally differentiating layers appeared to produce networks of bona fide 10–nm filaments. Thus, whether the differentiation program resulted in the expression of K1/K10 (epidermis), K6/K16 (ORS and tongue), or K3/K12 (cornea), suprabasal keratin filament networks assembled. In fact, the only tissue where we noted major differences in suprabasal IF networks was the esophagus, where the basal keratins persist throughout the K4/K13-containing suprabasal layers. Overall, these results demonstrate clearly that the K5/K14 network is not essential for the formation of most if not all differentiation-specific keratin networks. The results are consistent with those of Chan et al. (1994), but differ from those of Rugg et al. (1994), who reported that the K1 and K10 keratin network of suprabasal epidermal cells tended to form clumps or aggregates in a patient homozygous for a K14 premature stop codon mutation. It is possible that the genetic background of this individual contributed to an instability of the suprabasal keratin network. However, our studies show that clumping of keratin filaments suprabasally is not an inherent characteristic of K14 ablation. Thus, suprabasal keratin filaments do not require assembly upon a foundation of K5 and K14 filaments, as was first suggested by Kartasova et al. (1993). Whether the residual K5 and K15 network performs this function awaits ablation of the K5 or K15 gene.

A very special thank you goes to A. Syder for his expert assistance in art work. We thank Dr. D. Roop (Baylor University School of Medicine, Houston, TX) for his gift of anti-K6 antiserum. We thank Ms. A. Hansen for her expeditious assistance in the typing of this manuscript.

This work was supported by a grant from the National Institutes of Health (AR27883). E. Fuchs is an Howard Hughes Medical Institute investigator; C. Lloyd is a Fogarty International Scholar; K. Turksen is a Centennial Scholar supported by the Medical Research Council of Canada.

Received for publication 6 February 1995 and in revised form 24 February 1995.

#### *References*

Albers, K., and E. Fuchs. 1987. The expression of mutant epidermal keratin cDNAs transfected in simple epithelial and squamous cell carcinoma lines. *J. Cell Biol.* 105:791–806.

Anton-Lamprecht, I. 1983. Genetically induced abnormalities of epidermal differentiation and ultrastructure in ichthyoses and epidermolysis: pathogenesis, heterogeneity, fetal manifestation, and prenatal diagnosis. *J. Invest. Dermatol.* 81(Suppl.):149–156.

Anton-Lamprecht, I. 1994. Ultrastructural identification of basic abnormalities as clues to genetic disorders of the epidermis. *J. Invest. Dermatol.* (Suppl.): 103:65–125.

Bonifas, J. M., A. L. Rothman, and E. H. Epstein. 1991. Epidermolysis bullosa simplex: evidence in two families for keratin gene abnormalities. *Science (Wash. DC).* 254:1202–1205.

Byrne, C., and E. Fuchs. 1993. Probing keratinocyte and differentiation specificity of the K5 promoter in vitro and in transgenic mice. *Mol. Cell. Biol.* 13: 3176–3190.

Byrne, C., M. Tainsky, and E. Fuchs. 1994. Programming gene expression in developing epidermis. *Development (Camb.).* 120:2369–2383.

Chan, Y.-M., I. Anton-Lamprecht, Q.-C. Yu, A. Jackel, B. Zabel, J.-P. Ernst, and E. Fuchs. 1994. A human keratin 14 "knockout": the absence of K14 leads to severe epidermolysis bullosa simplex and a function for an intermediate filament protein. *Genes & Dev.* 8:2574–2587.

Cheng, J., A. J. Syder, Q. C. Yu, A. Letai, A. S. Paller, and E. Fuchs. 1992. The genetic basis of epidermolytic hyperkeratosis: a disorder of differentiation-specific epidermal keratin genes. *Cell.* 70:811–819.

Chipev, C. C., B. P. Korge, N. Markova, S. J. Bale, J. J. DiGiovanna, J. G. Compton, and P. M. Steinert. 1992. A leucine→proline mutation in the H1 subdomain of keratin 1 causes epidermolytic hyperkeratosis. *Cell.* 70:821–828.

Chomczynski, P., and N. Sacchi. 1987. Single-step method of RNA isolation by acid guanidinium thiocyanate-phenol-chloroform extraction. *Anal. Biochem.* 162:156–159.

Coulombe, P. A., M. E. Hutton, A. Letai, A. Hebert, A. S. Paller, and E. Fuchs. 1991*a*. Point mutations in human keratin 14 genes of epidermolysis bullosa simplex patients: genetic and functional analyses. *Cell.* 66:1301–1311.

Coulombe, P. A., M. E. Hutton, R. Vassar, and E. Fuchs. 1991*b*. A function for keratins and a common thread among different types of epidermolysis bullosa simplex diseases. *J. Cell Biol.* 115:1661–1674.

Fine, J.-D., E. A. Bauer, R. A. Briggaman, D.-M. Carter, R. A. Eady, N. B. Esterly, K. Holbrook, S. Hurwitz, L. Johnson, A. Lin, R. Pearson, and V. P. Sybert. 1991. Revised clinical and laboratory criteria for subtypes of inherited epidermolysis bullosa. *J. Am. Acad. Dermatol.* 24:119–135.

Franke, W. W., D. L. Schiller, M. Hatzfeld, and S. Winter. 1983. Protein complexes of intermediate-sized filaments: melting of cytokeratin complexes in urea reveals different polypeptide separation characteristics. *Proc. Natl. Acad. Sci. USA.* 80:7113–7117.

Fuchs, E. 1994. Intermediate filaments and disease: Mutations that cripple cell strength. *J. Cell Biol.* 125:511–516.

Fuchs, E., and H. Green. 1980. Changes in keratin gene expression during terminal differentiation of the keratinocyte. *Cell.* 19:1033–1042.

Fuchs, E., R. A. Esteves, and P. A. Coulombe. 1992. Transgenic mice expressing a mutant keratin 10 gene reveal the likely genetic basis for Epidermolytic Hyperkeratosis. *Proc. Natl. Acad. Sci. USA.* 89:6906–6910.

Fuchs, E., and K. Weber. 1994. Intermediate filaments: structure, dynamics, function, and disease. *Annu. Rev. Biochem.* 63:345–382.

Graham, F. L., and E. van der Eb. 1973. A new technique for the assay of infectivity of human adenovirus 5 DNA. *Virology.* 52:456–467.

Hanukoglu, I., and E. Fuchs. 1982. The cDNA sequence of a human epidermal keratin: divergence of sequence but conservation of structure among intermediate filament proteins. *Cell.* 31:243–252.

Hogan, B., R. Beddington, F. Constantini, and E. Lacy. 1994. Manipulating the mouse embryo. Cold Spring Harbor Laboratory Press, Cold Spring Harbor, NY. 1–497.

Kartasova, T., D. R. Roop, K. A. Holbrook, and S. H. Yuspa. 1993. Mouse differentiation-specific keratins 1 and 10 require a preexisting keratin scaffold to form a filament network. *J. Cell Biol.* 120:1251–1261.

Knapp, B., M. Rentrop, J. Schweizer, and H. Winter. 1987. Three cDNA sequences of mouse type I keratins. *J. Biol. Chem.* 262:938–945.

Kopan, R., and E. Fuchs. 1989. The use of retinoic acid to probe the relation between hyperproliferation-associated keratins and cell proliferation in normal and malignant epidermal cells. *J. Cell Biol.* 109:295–307.

Kulesh, D. A., and R. G. Oshima. 1988. Cloning of the human keratin 18 gene and its expression in nonepithelial mouse cells. *Mol. Cell. Biol.* 8:1540–1550.

Lane, E. B., E. L. Rugg, H. Navsaria, I. M. Leigh, A. H. M. Heagerty, A. Ishida-Yamamoto, and R. A. J. Eady. 1992. A mutation in the conserved helix termination peptide of keratin 5 in hereditary skin blistering. *Nature (Lond.).* 356:244–246.

Lersch, R., V. Stellmach, C. Stocks, G. Giudice, and E. Fuchs. 1989. Isolation, sequence, and expression of a human keratin K5 gene: transcriptional regulation of keratins and insights into pairwise control. *Mol. Cell. Biol.* 9:3685–3697.

Letai, A., P. A. Coulombe, M. B. McCormick, Q.-C. Yu, E. Hutton, and E. Fuchs. 1993. Disease severity correlates with position of keratin point mutations in patients with epidermolysis bullosa simplex. *Proc. Natl. Acad. Sci. USA.* 90:3197–3201.

Leube, R. E., B. L. Bader, F. X. Bosch, R. Zimbelmann, T. Achtstaetter, and W. W. Franke. 1988. Molecular characterization and expression of the stratification-related cytokeratin 4 and 15. *J. Cell Biol.* 106:1249–1261.

Mansbridge, J. N., and A. M. Knapp. 1987. Changes in keratinocyte maturation during wound healing. *J. Invest. Derm.* 89:253–262.

McCormick, M. B., P. Kouklis, A. Syder, and E. Fuchs. 1993. The roles of the rod end and the tail in vimentin IF assembly and IF network formation. *J. Cell Biol.* 122:395–407.

Moll, R., W. W. Franke, D. L. Schiller, B. Geiger, and R. Krepler. 1982*a*. The catalog of human cytokeratins: Patterns of expression in normal epithelia, tumors, and cultured cells. *Cell.* 31:11–24.

Moll, R., I. Moll, and W. Wiest. 1982*b*. Changes in the pattern of cytokeratin polypeptides in epidermis and hair follicles during skin development. *Differentiation.* 23:170–178.

Nelson, W., and T.-T. Sun. 1983. The 50- and 58-kdalton keratin classes as molecular markers for stratified squamous epithelia: cell culture studies. *J. Cell Biol.* 97:244–251.

Reis, A., H. C. Hennies, L. Langbein, M. Digweed, D. Mischke, M. Drechsler, E. Schrock, B. Royer-Pokora, W. Franke, K. Sperling, and W. Kuster. 1994. Keratin 9 gene mutations in epidermolytic palmoplantar keratoderma (EPPK). *Nature Genetics.* 6:174–179.

Rentrop, M., B. Knapp, H. Winter, and J. Schweizer. 1986. Differential localization of distinct keratin mRNA-species in mouse tongue epithelium by in situ hybridization with specific cDNA probes. *J. Cell Biol.* 103:2583–2591.

Roop, D. R., H. Huitfeldt, A. Kilkenny, and S. H. Yuspa. 1987. Regulated expression of differentiation-associated keratins in cultured epidermal cells detected by monospecific antibodies to unique peptides of mouse epidermal keratins. *Differentiation.* 35:143–150.

Rosenberg, M., A. RayChaudhury, T. B. Shows, M. M. LeBeau, and E. Fuchs. 1988. A group of type I keratin genes on human chromosome 17: characterization and expression. *Mol. Cell. Biol.* 8:722–736.

Rothnagel, J. A., A. M. Dominey, L. D. Dempsey, M. A. Longley, D. A. Greenhalgh, T. A. Gagne, M. Huber, E. Frenk, D. Hohl, and D. R. Roop. 1992. Mutations in the rod domains of keratins 1 and 10 in epidermolytic hyperkeratosis. *Science (Wash. DC).* 257:1128–1130.

Rugg, E. L., W. H. I. McLean, E. B. Lane, R. Pitera, J. R. McMillan, P. J. C. Dopping-Hepenstal, H. A. Navsaria, I. M. Leigh, and R. A. J. Eady. 1994. A functional "knockout" of human keratin 14. *Genes & Dev.* 8:2563–2573.

Schermer, A., S. Galvin, and T-T. Sun. 1986. Differentiation-related expression of a major 64K corneal keratin in vivo and in culture suggests limbal location of corneal eptiehlial stem cells. *J. Cell Biol.* 103: 49–62.

Schweizer, J., M. Kinjo, G. Furstenberger, and H. Winter. 1984. Sequential expression of mRNA-encoded keratin sets in neonatal mouse epidermis: Basal cells with properties of terminally differentiating cells. *Cell.* 37:159–170.

Schweizer, J., M. Rentrop, R. Nischt, M. Kinjo, and H. Winter. 1988. The intermediate filament system of the keratinizing mouse forestomach epithelium: coexpression of keratins of internal squamous epithelia and of epidermal keratins in differentiating cells. *Cell Tissue Res.* 253:221–229.

Stellmach, V., A. Leask, and E. Fuchs. 1991. Retinoid-mediated transcriptional regulation of keratin genes in human epidermal and squamous cell carcinoma cells. *Proc. Natl. Acad. Sci. USA.* 88:4582–4586.

Stoler, A., R. Kopan, M. Duvic, and E. Fuchs. 1988. The use of monospecific antibodies and cRNA probes reveals abnormal pathways of terminal differentiation in human epidermal diseases. *J. Cell Biol.* 107:427–446.

Sun, T.-T., R. Eichner, A. Schermer, D. Cooper, W. G. Nelson, and R. A. Weiss. 1984. The Transformed Phenotype. *In* The Cancer Cell. Vol. 1. A. Levine, W. Topp, G. van de Woude, and J. D. Watson, editors. Cold Spring Harbor Laboratory, Cold Spring Harbor, NY. 169–176.

Torchard, D., C. Blanchet-Bardon, O. Serova, L. Langbein, S. Narod, N. Janin, A. F. Goguel, A. Bernheim, W. W. Franke, G. M. Lenoir, and J. Feunteun. 1994. Epidermolytic palmoplantar keratoderma cosegregates with a keratin 9 mutation in a pedigree with breast and ovarian cancer. *Nat. Genet.* 6:106–109.

van Muijen, G. N. P., D. J. Ruiter, W. W. Franke, T. Achtstatter, W. H. B. Haasnoot, M. Ponec, and S. O. Warnaar. 1986. Cell type heterogeneity of cytokeratin expression in complex epithelia and carcinomas as demonstrated by monoclonal antibodies specific for cytokeratins nos 4 and 13. *Exp. Cell Res.* 162:97–113.

Vassar, R., P. A. Coulombe, L. Degenstein, K. Albers, and E. Fuchs. 1991. Mutant keratin expression in transgenic mice causes marked abnormalities resembling a human genetic skin disease. *Cell.* 64:365–380.

Webster, K. A. 1987. Regulation of glycolytic enzyme transcriptional rates by oxygen availability in skeletal muscle cells. *Mol. Cell Biochem.* 17:19–28.

Warhol, M. J., J. M. Lucocq, E. Carlemalm, and J. Roth. 1985. Ultrastructural localization of keratin proteins in human skin using low-temperature embedding and the protein A-gold technique. *J. Invest. Dermatol.* 84:69–72.

Wu, R. L., Z. Guoung, S. Godvin, C. Xu, T. Haseba, C. Chaloin-Dufau, D. Dhouailly, Z.-G. Wei, R. M. Lavker, W.-Y. Kao, and T. T. Sun. 1994. Lineage-specific and differentiation dependent expression of K12 keratin in rabbit corneal/limbal epithelial cells: cDNA cloning and northern blot analysis. *Differentiation.* 55:137–144.

Wu, Y.-J., L. M. Parker, N. E. Binder, M. A. Beckett, J. H. Sinard, C. T. Griffiths, and J. G. Rheinwald. 1982. The mesothelial keratins: a new family of cytoskeletal proteins identified in cultured mesothelial cells. *Cell.* 31:693–703.